

## Hairpin Configurations of Triblock Copolymers at Homopolymer Interfaces

T. P. Russell,\* A. M. Mayes, and V. R. Deline

IBM Research Division, Almaden Research Center, 650 Harry Road,  
San Jose, California 95120-6099

T. C. Chung

Department of Materials Science and Engineering, The Pennsylvania State University,  
University Park, Pennsylvania 16802

Received March 2, 1992; Revised Manuscript Received June 17, 1992

**ABSTRACT:** The organization of triblock copolymers containing a central block of polystyrene (PS) and two outer blocks of poly(methyl methacrylate) (PMMA), denoted P(MMA-*b*-S-*b*-MMA), at the interface of immiscible homopolymers was investigated by dynamic secondary ion mass spectrometry. Selective labeling of either the two end blocks or the central block provided the contrast necessary to determine the spatial arrangements of the blocks at the interfaces. Triblock copolymers at the interface between PS and poly(vinyl chloride) (PVC), poly(2,6-dimethylphenylene oxide) (PXE) and PVC, and PXE and PMMA were investigated. In all cases it was found that the triblock copolymers were organized such that the central block preferentially segregated to one homopolymer whereas the end blocks segregated to the other forming a "hairpin" type of conformation. For different triblock copolymer concentrations, essentially the same distribution of segments at the interface is found, differing only by a scaling factor. Adding excessive amounts of the triblock to the interface, however, causes a substantial broadening, which suggests aggregation of the copolymers at the interface. In comparison to P(S-*b*-MMA) diblock copolymers of equal molecular weight and composition, the triblock copolymer at lower concentrations produces a larger broadening of the interface. However, for concentrations approaching half the copolymer period, the interfacial broadening for the two cases is similar. In addition, although the central PS block of the triblock is anchored to the interface at both ends, the extension of this block away from the interface is very similar to that seen for the PS block of the corresponding diblock copolymer.

### Introduction

Miscibility of two polymers is the exception rather than the rule. Due to the small entropic gains in mixing two polymers, relatively small unfavorable interactions between unlike monomers will generally result in a macroscopic separation of the two components. The extent of phase separation can be limited, however, by the use of diblock copolymers which serve to reduce the interfacial tension between the phases formed, thereby permitting a finer dispersion of the two components.<sup>1,2</sup> The size scale of the phase separation will depend upon the concentration of the diblock copolymer used as the compatibilizing agent.

It is now well established that, for an A-B diblock copolymer where block A is miscible with one homopolymer and block B with the other, the copolymer bridges between the two homopolymer phases, with the copolymer junction points residing preferentially at the interface between the two homopolymers.<sup>3-8</sup> In the case of an A-B diblock copolymer in the presence of A and B homopolymers, it has been shown that a planar interface becomes saturated with copolymer chains when essentially a monolayer (the equivalent of half the copolymer period) of the diblock is placed at the interface.<sup>6</sup> The copolymer induces a broadening of the interface between the A and B components which is in keeping with a reduction in the interfacial tension. The extent of penetration of the homopolymer into the interfacial region will depend upon the ratio of the molecular weight of the block to that of the homopolymer.<sup>9,10</sup> For a fixed block molecular weight, the homopolymer penetration decreases with increasing homopolymer molecular weight. The addition of more than a monolayer of the diblock copolymer results in the formation of ordered copolymer structures at the interface in the form of micelles.<sup>6,7</sup>

In addition to improving the compatibility of bulk homopolymer mixtures, diblock copolymers at an interface between immiscible homopolymers will enhance the adhesion between the two homopolymer phases.<sup>4</sup> The increase in adhesion will depend upon the extent of interpenetration of the homopolymer and copolymer segments and the ease with which the copolymer can be pulled out or disentangled from the homopolymer phase.<sup>11</sup> One possible means of increasing chain entanglement is by use of a triblock or multiblock copolymer. Here, provided the copolymers order at the interface between the homopolymers, the loops of the copolymer blocks are anchored at the interface between the homopolymers. The loops extend into the homopolymer phase, entangle with the homopolymer chains, and effectively stitch the two homopolymers together.

However, little is known concerning the ordering of multiblock copolymers at homopolymer interfaces. While it is easy to visualize this looped arrangement, no real proof exists in the literature that multiblock copolymers order at interfaces. In this article a dynamic secondary ion mass spectrometry, DSIMS, study is presented which demonstrates, by selective deuteration of blocks of an ABA type triblock copolymer, that ordering of the triblock copolymer at immiscible homopolymer interfaces occurs. As observed with diblock copolymer additions, a saturation of the interface is found to occur when more than a monolayer of the triblock copolymer is placed at the interface. It is also shown that, to within the resolution limits of DSIMS, the extension of the blocks, be they anchored at one or both ends to the interface, is essentially the same. Below the saturation limit, however, the data indicate that triblock copolymers induce a greater broadening of the interface compared with diblock copolymers of equal composition and molecular weight. This suggests

Table I  
Characteristics of Triblock Copolymers

	$(M_w)_{PS}$	$(M_w)_c^a$	$(M_w/M_n)_c^b$
P(MMA- <i>b</i> -d-S- <i>b</i> -MMA)	62 000	125 000	1.49
P(d-MMA- <i>b</i> -S- <i>b</i> -d-MMA)	50 000	100 000	1.50
P(d-S- <i>b</i> -MMA) <sup>c</sup>	52 000	100 000	1.03

<sup>a</sup>  $(M_w)_c$  is the total molecular weight of the copolymer. <sup>b</sup>  $(M_w/M_n)_c$  is the polydispersity of the triblock copolymer. <sup>c</sup> Purchased from Polymer Laboratories and Soxhlet-extracted in cyclohexane before use.

that, for an unsaturated interface, the triblock architecture is more effective at reducing interfacial tension.

## Experimental Section

Triblock copolymers containing a central polystyrene block with two outer blocks of poly(methyl methacrylate), denoted P(MMA-*b*-S-*b*-MMA), were prepared by use of the difunctional initiator disodium dibenzyl anion, which was generated in situ at the beginning of the polymerization. The entire reaction was performed within two 500-mL flasks attached to a high-vacuum apparatus.<sup>12</sup> In a typical example, naphthalene (128 mg) was mixed with an excess of sodium (200 mg) in one flask. Dry tetrahydrofuran (THF; 300 mL) was introduced to this mixture by vacuum distillation. After the complete formation of sodium naphthalide (~1 mmol), the light green solution was transferred to the second flask. Styrene monomer (15.3 g) was then vacuum distilled into the reactor flask. Immediately, sodium naphthalide reacted with the styrene monomer to form the radical anion which then dimerized via a tail-tail radical coupling reaction to form the disodium dibenzyl anion.<sup>13</sup> This dianion constituted the initiator for the living anionic polymerization of the styrene monomer. To ensure complete conversion, the polymerization reaction was allowed to proceed at room temperature for 6 h. The solution was then cooled to -78 °C before vacuum distilling purified methyl methacrylate monomer (14.7 g) into the reaction vessel. After 5 h, the polymerization was terminated by the addition of methanol (5 mL) under vacuum. The triblock copolymer was precipitated in isopropyl alcohol and dried under vacuum. In synthesizing copolymers with labeled blocks, the appropriate perdeuterated monomer was used.

The triblock copolymers were characterized by size-exclusion chromatography coupled with UV/visible detectors to measure the molecular weights of both the central styrene block and the total copolymer. The molecular weights of the methyl methacrylate blocks were assumed to be identical. The characteristics of the triblock copolymers are given in Table I. As can be seen, the molecular weight distributions of the triblock copolymers are fairly narrow and the fractions of the two components in the copolymer are essentially equal. For a triblock copolymer this means that the molecular weight of the central block is twice that of the end blocks.

The polystyrene (PS) and poly(methyl methacrylate) (PMMA) homopolymers used in this study were purchased from Polymer Laboratories and had weight-average molecular weights of  $9.6 \times 10^4$  and  $1.07 \times 10^5$ , respectively. From size-exclusion chromatography, in reference to polystyrene and poly(methyl methacrylate) standards, the polymers had polydispersities of 1.05 and 1.03, respectively. The poly(2,6-dimethylphenylene oxide) or poly(xylinyl ether), denoted PXE, was obtained from General Electric Laboratories and had a weight-average molecular weight of  $3 \times 10^4$  with  $M_w/M_n = 2.0$ . The poly(vinyl chloride) (PVC) obtained from Polysciences had an  $M_w \sim 3 \times 10^4$  with  $M_w/M_n \sim 2.0$ . All homopolymers were used as received.

A Perkin-Elmer PHI 6300 secondary ion mass spectrometer was used to acquire the DSIMS depth profiles from the polymer films. A 216-nA, 2-keV  $O_2^+$  primary ion beam at an angle of incidence of 60° from the surface normal provided the sputtering. The primary ion beam was rastered at either  $400 \times 400 \mu m^2$  or at  $550 \times 550 \mu m^2$ , and negative secondary ions of  $^1H^-$ ,  $^2D^-$ ,  $^{12}C^-$ ,  $^{16}O^-$ ,  $^{26}CN^-$ , and  $^{35}Cl^-$  were measured from the center 20% of the full raster. An electron beam was used for charge compensation.

Trilayer polymer films were prepared as specimens for the dynamic secondary ion mass spectroscopy, DSIMS, experiments.

First, a solution of PMMA in toluene or PVC in THF was placed on the surface of a 2.5-cm-diameter quartz wafer mounted on a standard photoresist spin-coating device. Spinning the wafer drives off excess solution, leaving behind a thin polymer film. Films of  $\sim 10^3$  Å in thickness were achieved by adjusting the solution concentration or the spinning speed. On a  $7.5 \times 12.5$  cm<sup>2</sup> microscope slide, a film of the triblock copolymer with a specified thickness was prepared in a similar manner. The sides of the slide were scored with a razor blade, and the film was floated off onto a pool of distilled water. For cases where PMMA was the initial film, a trace amount of table salt was dissolved in the water, so that the Cl signal could be used as a marker for this interface. The film floating on the surface was retrieved with the coated quartz substrate, and the bilayer was heated to 80 °C for 1/2 h to drive off the water and to relax the copolymer film. Without performing this minimal annealing, subsequent dipping of the bilayer in water could cause the triblock layer to lift off the surface. In a similar manner, a film of either PS or PXE  $\sim 0.1 \mu m$  thick was cast on a microscope slide, floated onto a pool of water, and transferred onto the bilayer, thereby forming a trilayered specimen.

All the trilayers were annealed at 180 °C for 240 h under vacuum. While PVC can dehydrochlorinate at lower temperatures, no evidence of this was observed in the sample preparation. Typically, trace amounts of dehydrochlorination, due to removal of HCl from consecutive monomers, produce a conjugated double-bond sequence which is quite evident by an intense discoloration of the film.<sup>14</sup> Observation of the film at different angles revealed no discoloration, and the strong Cl signal in the DSIMS gave further indication that substantial degradation of the PVC did not occur. While it is possible that some degradation may have occurred, the effects should not be of significance in the framework of these experiments. After the trilayer samples were annealed, a thin ( $\sim 200$  Å) layer of perdeuterated polystyrene was transferred onto the surface by the method described above. This film served as a buffer layer in which the sputtering transition to a constant sputtering rate was achieved and served as a convenient marker for the air surface.

The annealing temperature is also well below the glass transition temperature,  $T_g$ , of the PXE, which is  $\sim 210$  °C. This, however, should not substantially perturb the triblock diffusion at the interface since locally the  $T_g$  for PS volume fractions greater than  $\sim 0.3$  is equal to or less than the annealing temperature. For bilayer specimens of PS and PXE annealed at temperatures as low as 160 °C, substantial interdiffusion is seen.<sup>15,16</sup> Thus, while the motions may be slowed down by the relatively high  $T_g$  of the PXE, it should still be possible for the copolymer to reorganize at the interface into a nearly equilibrium conformation.

## Results and Discussion

A typical example of a DSIMS profile is shown in Figure 1 for a trilayered specimen of PXE/P(MMA-*b*-d-S-*b*-MMA)/PVC, where a triblock copolymer film with a thickness corresponding approximately to one-quarter of the triblock lamellar period was placed at the interface. The signals arising from  $^{35}Cl^-$ ,  $^{12}C^-$ ,  $^1H^-$ ,  $^2H^-$ , and  $^{26}CN^-$  are plotted as a function of depth. The profiles have been vertically offset for clarity. There are several features of these data which are important to mention for the subsequent discussion. These are detailed below.

First, the data as collected in the DSIMS experiment are obtained as a function of the sputtering cycle or time. In order to place the data on a depth scale, it is necessary to multiply the sputtering time by the appropriate sputtering rate. It was arbitrarily assumed that the sputtering rate was equal to the experimentally obtained sputtering rate for polystyrene of 3.9 Å/s, independent of the polymer through which the ion beam was sputtering. The sputtering rates in the different polymers are not the same, however. Under the conditions in which the DSIMS was performed the sputtering rate is 3.9 Å/s in PS, 5.5 Å/s in PXE, 5.5 Å/s in PVC, and 8.0 Å/s in PMMA.

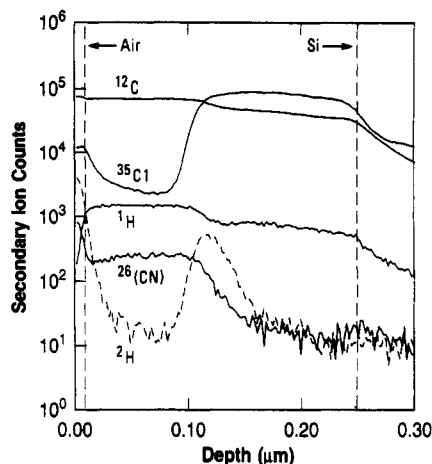


**Figure 1.** Typical example of dynamic secondary ion mass spectrometry profiles from a trilayer of PXE/P(MMA-*b*-S-*b*-MMA)/PVC where the secondary ion counts are shown as a function of depth for  $^{12}\text{C}$ ,  $^{35}\text{Cl}$ ,  $^1\text{H}$ ,  $^{26}(\text{CN})^-$ , and  $^2\text{H}$ . The profiles have been offset vertically for clarity. The vertical dashed lines indicate the positions of the air and substrate interfaces where a depth of zero is the air surface.

In order to account properly for the variation in the sputtering rate as the ion beam penetrates into the interfacial region, a systematic variation in the sputtering rate as a function of the composition of the components (minimally three different components for the cases investigated here) could be determined experimentally. Using this matrix of sputtering rates and assuming a composition profile across the interface, then one could, incorporating the instrumental resolution, calculate the expected DSIMS profiles and compare them to the experimental data. While this is, in principle, possible, the number of assumptions required in the calculation would place severe restrictions on the interpretations. Consequently, albeit incorrect, a constant sputtering rate was assumed. While this assumption limits the quantitative interpretation of the spatial distribution of the segments or the extent to which chains are stretched at the interface, the major conclusion of this work, i.e., the manner in which the triblock copolymers organize at the interface, will not be altered. In addition, since the lowest sputtering rate was used for the conversion, the distances reported in PXE, PVC, and PMMA will be shorter than the actual distances.

The air/polymer and polymer/substrate interfaces are indicated in the figure by the vertical dashed lines. Determination of these interfaces is relatively straightforward from the abrupt changes in the signals of the different components. At the original air surface the signals arising from  $^2\text{H}$ ,  $^{35}\text{Cl}$ ,  $^{26}(\text{CN})^-$ , and  $^1\text{H}$  undergo marked changes. The variation in the  $^2\text{H}$  and  $^1\text{H}$  signals can be understood from the change in going from the d-PS overlayer to the PXE upperlayer of the trilayer. The variation in the  $^{35}\text{Cl}$  and  $^{26}(\text{CN})^-$  arises from the fact that any impurities in the water used to transfer the upper film would give rise to pronounced signals of these masses. It should be recalled that, after transfer of this buffer layer, no annealing was performed and, consequently, there could be a relatively high concentration of impurities at this interface. In addition, DSIMS is very sensitive to these two masses, and, therefore, such changes are not surprising. It should be noted that decay of the  $^{35}\text{Cl}$  signal into the upper layer is rather broad, which may indicate that the area selected for the analysis contained a slight imperfection such as a crack or pinhole in which small amounts of chlorine-containing impurities could have been trapped.

Such an effect is magnified by the sensitivity of DSIMS to  $^{35}\text{Cl}$ .

The precise location of the interface formed between the two polymers in the trilayer, however, is somewhat difficult if not impossible to determine by one isolated measurement. Changes in the  $^1\text{H}$ ,  $^{12}\text{C}$ ,  $^{35}\text{Cl}$ , and  $^{26}(\text{CN})^-$  signals are clearly evident which provide a convenient means of aligning successive DSIMS profiles. Due to the presence of the copolymer, however, these do not correspond to the location of the interface. The variation in the  $^1\text{H}$  and  $^{12}\text{C}$  signals arises from the changes in the density of  $^1\text{H}$  and  $^{12}\text{C}$  between the two components and to the yield of the ions as the sputtering rate changes in going from one component to the next. In the case of PXE, a strong signal at a mass of 26 is observed which can be attributed to trace quantities of catalysts or stabilizers containing nitrogen. DSIMS is exceptionally sensitive to  $^{26}(\text{CN})^-$ , and, consequently, assigning this signal to nitrogen is quite reasonable. Nonetheless, this signal serves as a very convenient marker for the PXE layer in the specimen. The relatively sharp rise in the  $^{35}\text{Cl}$  signal for the PVC clearly distinguishes the interface between PVC and the remainder of the components in the trilayer. The sensitivity of DSIMS for  $^{35}\text{Cl}$  and the magnitude of this signal provides an excellent means of comparing different DSIMS profiles. For all the cases studied here, the only variable in comparing two different profiles is the labeling of the triblock copolymer, namely, deuterated end or center blocks. Thus by shifting the  $^{35}\text{Cl}$  or  $^{26}(\text{CN})^-$  signals so that they are coincident and offsetting the depth scales for the  $^2\text{H}$  signals, this same amount provides a direct means of comparing the spatial distribution of the copolymer blocks. The beauty of this is that, independent of any errors in the assumed sputtering rates, such an offsetting procedure eliminates the need of knowing the precise thickness of the layers and the exact position of the interface. Thus, even if the data were kept on a time scale, without any assumptions, the DSIMS measurements yield a direct answer to the organization of the triblock at the interface.

The signal arising from the portion of the triblock copolymer labeled with deuterium is clear. Whether the PS or PMMA blocks of the triblock copolymer were labeled, in the range where the  $^{12}\text{C}$ ,  $^{35}\text{Cl}$ ,  $^1\text{H}$ , and  $^{26}(\text{CN})^-$  signals undergo a change, a strong maximum in the  $^2\text{H}$  signal is observed. By offsetting the depth scales such that the changes in the  $^{35}\text{Cl}$  or  $^{26}(\text{CN})^-$  signals are coincident, the variation in the  $^2\text{H}$  signal from successive experiments, where the labeling or concentration of the triblock copolymer has been changed, can be placed on a common scale. This type of alignment allows an independent assessment of the triblock copolymer ordering without knowing a priori the position of the interface. Thus, two DSIMS experiments are performed on identical systems with the exception that the labeling of the copolymer is changed. Without any assumptions the two profiles can be offset in the depth scale and the profiles of the  $^2\text{H}$  arising from the different portions of the copolymer which are labeled can be compared. An ordering of the copolymer will be directly seen by a displacement of the signal arising from the deuterium labels. After offsetting the  $^2\text{H}$  signals, as will be seen, the approximate position of the interface is evident. All DSIMS profiles were offset in this manner, and, henceforth, only the  $^2\text{H}$  profile will be presented.

Shown in Figure 2 are the  $^2\text{H}$  signals observed for the cases where P(MMA-*b*-d-S-*b*-MMA) and P(d-MMA-*b*-S-*b*-d-MMA) were placed at the interface between PS and

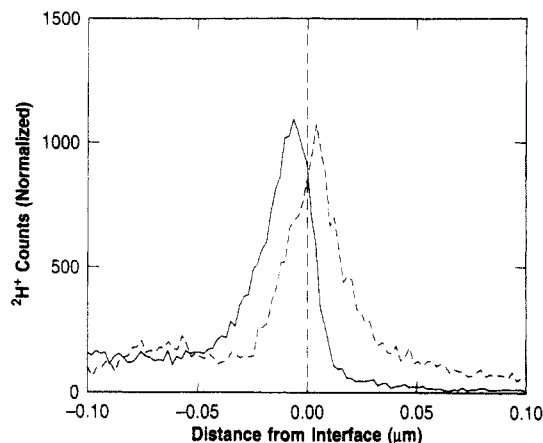


**Figure 2.**  $^2\text{H}$  profiles for two P(MMA-*b*-S-*b*-MMA) triblock copolymers at the interface between PS and PVC. The solid line is for P(MMA-*b*-d-S-*b*-MMA), and the dashed line is for P(d-MMA-*b*-S-*b*-d-MMA). The depth scale was offset as discussed in the text, and the vertical dashed line indicates the position of the interface between the layers. The total amount of copolymer placed between the PS and PVC corresponds to  $0.4L$  where  $L$  is the period of the lamellar morphology of the copolymer.

PVC. Using the offset procedure just discussed, it is evident that the  $^2\text{H}$  signals reach a maximum at different depths. Without further treatment of the data, these results show that the triblock copolymer has ordered at the interface between the PS and PVC. More specifically, the PS portion of the triblock segregates to the PS homopolymer layer, whereas the PMMA end blocks of the copolymer reside within the PVC layer. Given the favorable interactions between the PMMA and PVC segments<sup>17</sup> and the immiscibility of PS with PVC and PMMA with PS, these data confirm that the triblock must be organized in a hairpin type of configuration at the interface.

An indication of the approximate position of the interface is given by a vertical dashed line drawn at the position where the two signals maximally overlap. The depth scale was then normalized to zero at this point, with negative numbers indicating the PS side and positive the PVC side of the interface. It should be noted that the  $^2\text{H}$  signals arising from the PS center block and the PMMA end blocks reach a maximum away from the interface. This is to be expected when one considers that PVC and PMMA segments extend into the PS side of the interface and, conversely, PS segments from the homopolymer and copolymer extend into the PVC side of the interface. In fact, the distance between the positions of the maxima of the  $^2\text{H}$  signals from the PS and PMMA blocks serves as a measure of the interfacial width.

If one considers that the sputtering rate in PVC is 80% slower than in PS, then the distance between the two maxima in the  $^2\text{H}$  signals is more like  $140 \pm 30$  Å. Regardless of this difference, the interface measured by DSIMS between PS and PVC in the absence of the triblock copolymer is  $30 \pm 10$  Å. Consequently, the addition of the triblock copolymer has resulted in a dramatic broadening of the interface between the PS and PVC.

A note should be made on the precision to which the interface can be measured. As mentioned, the width of the interface was estimated by the separation distance between the maxima of the  $^2\text{H}$  signals. Even though a sharp interface can be broadened 130 Å by instrumental smearing as shown previously,<sup>18</sup> the convolution of the smearing function with the  $^2\text{H}$  profiles will not change the spatial position of the maximum. Consequently, while the full width of the  $^2\text{H}$  signal will be broadened, its position

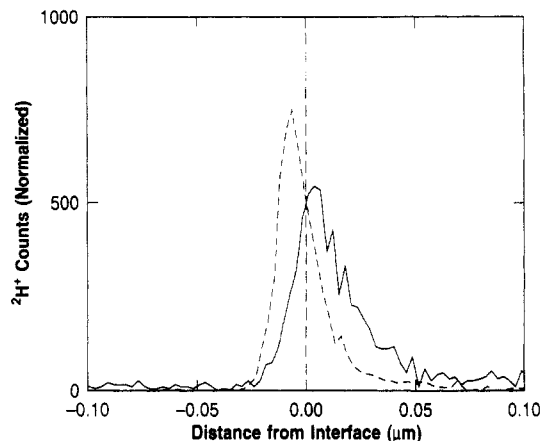


**Figure 3.**  $^2\text{H}$  profiles for trilayers of PXE/P(MMA-*b*-S-*b*-MMA)/PVC where the styrene block is labeled with deuterium (---) and where the methylmethacrylate block is labeled with deuterium (—). The depth scale was offset as described in the text, and the vertical dashed line indicates the position of the interface. Negative values correspond to the PXE side of the interface and positive to the PVC side.

will be invariant provided the resolution function is symmetric. Since the compositions of three components are varying as the interface is crossed, the resolution function may, in fact, not be symmetric. It is precisely this asymmetry which introduces the maximum error. The limits of  $\pm 30$  Å as stated above are well outside of any errors and serve as a very conservative estimate.

The full widths at half-maximum (fwhm) for the  $^2\text{H}$  signals from the PS block and PMMA end blocks are virtually identical at 260 Å. Caution must be exerted in interpreting this value as the distance over which the PS or PMMA segments of the copolymer are distributed in space. Convolved into this is the depth resolution function of the DSIMS. In addition, the differences of sputtering rates in PS and PVC would underestimate the width of the spatial distribution of PMMA. However, if one considers the molecular weights of the blocks and the hairpin configuration required to obtain these results, it appears that both the PS and PMMA blocks are stretched at the interface. For a PS chain with a molecular weight of 50 000 anchored at both ends to a solid surface, one would expect the unperturbed chain to span  $\sim 80$  Å,<sup>19</sup> which is significantly smaller than the PS block distribution observed in Figure 2. Since the PS segments of the triblock copolymer do not encounter strong favorable interactions with the PS homopolymer segments, any substantial stretching of the central PS block must be associated with a crowding of the junction points at the interface arising from the strong favorable interactions of the PMMA segments of the copolymer and the PVC homopolymer.

The organization of P(MMA-*b*-S-*b*-MMA) triblock copolymer at the interface between two immiscible homopolymers is also seen in the case where PS is substituted with PXE. Here, the PS block is miscible with PXE<sup>20</sup> and the PMMA block with PVC. Thus, one would expect that the PS segments would reside predominantly on the PXE side of the interface and PMMA on the PVC side. The  $^2\text{H}$  signals from the differently labeled triblock copolymers are shown in Figure 3. As in the previous case, one sees the  $^2\text{H}$  signal from the PS center block reaching a maximum at a depth different from that of the  $^2\text{H}$  signal arising from the PMMA end blocks. Once again, the triblock must assume a hairpin type of configuration to produce the results shown. Even though the annealing temperature of 180 °C is well below the  $T_g$  of PXE, there

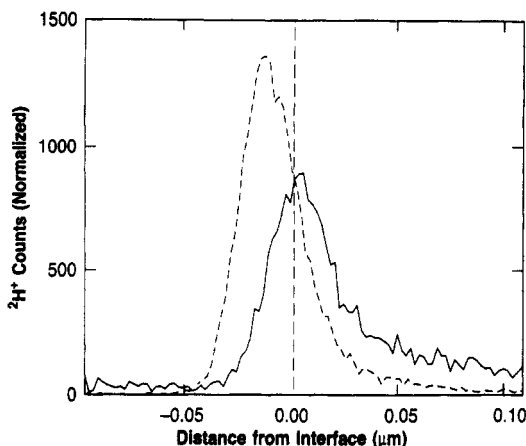


**Figure 4.**  $^2\text{H}$  profiles for trilayers of PXE/P(MMA-*b*-S-*b*-MMA)/PVC where the styrene block is labeled with deuterium (---) and where the methyl methacrylate is labeled with deuterium (—). The amount of triblock copolymer added was in excess of  $0.5L$ . The depth scale was offset as described in the text, and the vertical dashed line corresponds to the approximate position of the interface.

is sufficient mobility at the interface to allow the triblock copolymer to organize. This is not surprising, since experiments by Composto and Kramer<sup>15</sup> along with results from our own studies<sup>16</sup> have shown that substantial interdiffusion of PS into PXE can occur even at temperatures as low as 160 °C.

An interesting difference arises in comparing the PXE/PVC results in Figure 3 with those obtained for PS/PVC in Figure 2. In the latter case, the  $^2\text{H}$  signals from the PS and PMMA blocks are approximately symmetric as a function of depth. However, in the PXE/PVC case, a distinct asymmetry is observed. The fwhm's of the PS and PMMA signals in this case are 180 and 260 Å, respectively, compared with 260 Å for both blocks in the case of PS/PVC. This stands in apparent contradiction to the fact that PS is miscible with PXE, and one would expect, if anything, that the PS segments would be more stretched in the PXE than in the PS. This discrepancy results primarily from the assumed invariance of the sputtering rate for the different polymers. The sputtering rate in PS is 3.9 Å/s, whereas in PXE the sputtering rate is 5.5 Å/s. The ratio of the two sputtering rates is 1.4 which, when multiplied by 180 Å, yields a corrected fwhm of  $\sim 250$  Å, virtually the same as that seen for the PS/PVC case. The difference in the sputtering rates can, also, result in a difference in the ion yields between the two polymers and a distortion of the apparent spatial distribution of the  $^2\text{H}$  signal when comparing the two different cases. Thus, it is difficult to assess quantitatively the extent of stretching of the PS center block in the PXE layer without adjusting for the different sputtering rates. Still, the organization of the triblock at the interface is clear, and the interface between the two layers, based on the position of the maxima of the  $^2\text{H}$  signals, is at least 100 Å, much broader than that between PXE and PVC layers in the absence of the triblock copolymer, where an interfacial width of  $30 \pm 10$  Å was found.

If the amount of copolymer at the interface is increased, i.e., if the thickness of the copolymer layer is increased, so that the total amount of copolymer exceeds a monolayer coverage, then the profiles of the  $^2\text{H}$  signals from the PS and PMMA begin to broaden substantially. For example, Figure 4 shows the case of PXE/PVC where the copolymer layer is somewhat thicker than half the triblock period. In comparison to Figure 3 it is seen that both the PS and PMMA signals have broadened considerably. While there

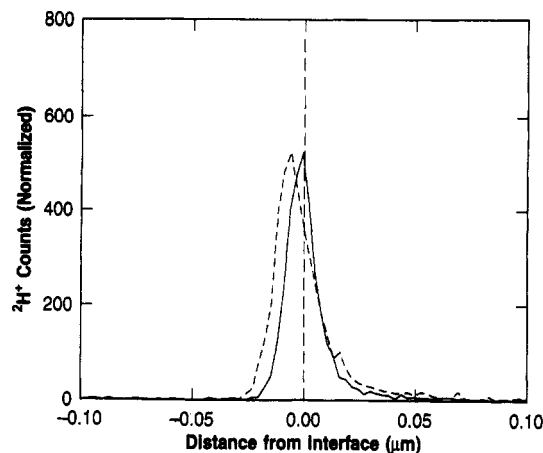


**Figure 5.**  $^2\text{H}$  counts as a function of distance from the interface (indicated by the dashed vertical line) comparing the signal arising from the PS block of a P(d-S-*b*-MMA) diblock (—) and P(MMA-*b*-d-S-*b*-MMA) triblock (---) copolymer of equal total molecular weights and styrene fractions. Here, a film corresponding to  $0.2L$  was placed at the interface between PXE and PVC.

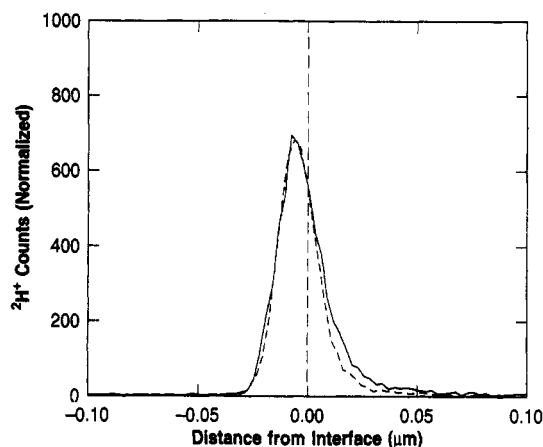


**Figure 6.** Same as Figure 5 but where a film of thickness  $0.4L$  was placed at the interface between PXE and PVC.

is still a tendency for the copolymer to arrange at the interface, the extent of overlap between the different blocks is quite large. Consequently, it is not possible to make any definitive statements on the details of the triblock ordering from these data alone. However, one may conclude that, upon adding an excess of copolymer to the interface, the simple hairpin description is evidently no longer applicable.

The behavior of P(MMA-*b*-S-*b*-MMA) triblock copolymer at an interface between PXE and PVC can be compared to that of the corresponding diblock copolymer. Results for placing copolymer films with thicknesses of  $0.2L$  and  $0.4L$ , where  $L$  is the repeat period of the lamellar morphology of the copolymer, are shown for the triblock and diblock copolymers in Figures 5 and 6, respectively. The characteristics of the diblock copolymer used in this study are given in Table I. The diblock copolymer had a total molecular weight of  $10^5$ , with PS and PMMA blocks of approximately equal molecular weights. Consequently, the total molecular weight of the copolymers, the molecular weight of the styrene block, and the fraction of styrene segments in the two copolymers were approximately equal. Obviously, the molecular weight of the methyl methacrylate block of the diblock is twice that of the end blocks in the triblock. For this reason, only the signals arising from the PS block will be discussed. The offset procedure of the diblock and triblock data was performed as described previously.

For a 0.2L layer thickness, the data in Figure 5 show that the  $^2\text{H}$  signal from the PS central block of the triblock (dotted line) reaches a maximum value further away from the interface than that from the PS block of the diblock copolymer (solid line). This result was quite surprising since it would be expected that the PS chain of the diblock would extend much further from the interface than the PS chain of the triblock which is anchored at two ends.<sup>19</sup> In addition, the styrene segment distribution is somewhat broader for the triblock.

These results suggest that, for the case where coverage of the copolymer at the interface is low, the triblock induces a greater broadening of the interface between the two layers. For equal molecular weights and concentrations, the triblock architecture appears to be more effective in reducing interfacial tension. When it is considered that for each triblock chain there are twice as many junction points as in the corresponding diblock copolymer, this result is quite reasonable. The entropic penalty for confining the copolymer junction points to an interface is smaller when the interfacial region is broader. For low coverages, one could argue that the reduction in interfacial tension effected by placing triblocks at the boundary between immiscible homopolymers would be comparable to that observed for the same concentration of diblocks of half the molecular weight.<sup>21</sup>

In general agreement with our findings, a recent Monte Carlo study by Balazs and co-workers suggests that linear  $(\text{AB})_n$  multiblock chains are more effective in decreasing the surface tension between immiscible liquids A and B than  $n$  AB diblocks.<sup>22</sup> An earlier mean-field analysis by Leibler, valid for slightly immiscible homopolymers A and B, also suggests that the interfacial region expands more upon adding  $(\text{AB})_n$  multiblocks versus an equal concentration of AB diblocks.<sup>23</sup>

For the PXE/PVC system, as the concentration of copolymer at the interface is increased to 0.4L, the  $^2\text{H}$  signals from the PS blocks of the two copolymers are virtually identical, as shown in Figure 6. From the interface between the two layers indicated by the dashed vertical line, the distribution of the PS segments reaches a maximum value at essentially the same distance into the PXE and only slight differences are seen on the PVC side of the interface. Thus, it can be concluded that the interfacial width and the extent to which the interfacial tension is reduced are basically the same in the two cases. The initial improvements attributed to the increased number of junction points are apparently nullified by other effects, such as crowding of the copolymer chains at the interface.

Up to this point, cases have been presented in which favorable interactions between the end blocks of the triblock copolymer and the adjacent homopolymer layer serve as a strong driving force for the triblocks to order at the interface. By contrast, in the case of the triblock copolymer at the interface between PXE and PMMA, the PS center blocks interact favorably with the PXE, whereas the interactions between the end blocks and the PMMA homopolymer are weaker. As shown in Figure 7, however, this interaction is still sufficient to cause an ordering of the triblock copolymer. Here the  $^2\text{H}$  signals from the PS and PMMA blocks are shown as a function of distance from the interface. In comparison to Figure 5, the  $^2\text{H}$  signal from the PS block has the same spatial distribution as that seen in the PXE/PVC case. Unfortunately, the signal arising from the PMMA end blocks of the copolymer is severely distorted by the sensitivity of PMMA to the ion beam. While it is clear that the  $^2\text{H}$  signal from the

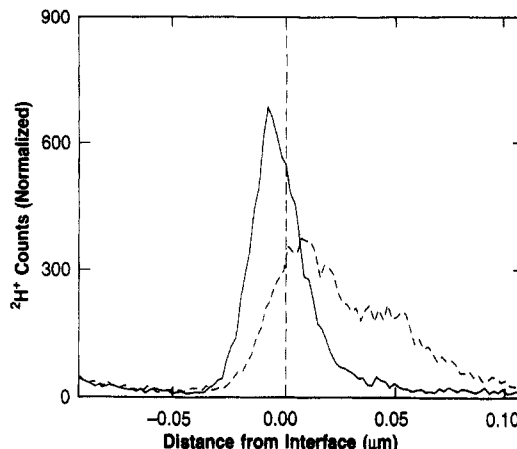


Figure 7.  $^2\text{H}$  counts for the PS (—) and PMMA (---) blocks of a P(MMA-*b*-S-*b*-MMA) triblock copolymer at the interface (indicated by the vertical dashed line) between PXE and PMMA. A film of P(MMA-*b*-S-*b*-MMA) corresponding to 0.4L was placed between layers of PXE and PMMA.

PMMA block attains a maximum value on the PMMA side of the interface, it is impossible to say anything further. This loss in sensitivity is reflected by the fact that the signal from the PMMA block is seen at distances of over 500 Å from the interface and, in fact, appears to plateau up to this distance. Given the signal observed for the PS center block, it is impossible for the signal from the PMMA end blocks to extend out to such distances from the interface. This must, therefore, be an artifact associated with the degradation of the PMMA in the ion beam. Consequently, the only statement that can be made is that the triblock orders at the interface and assumes a hairpin configuration.

One outstanding question which remains is whether the triblock copolymer would order at the interface between two immiscible homopolymers in the absence of any strong favorable interactions. For P(MMA-*b*-S-*b*-MMA), the obvious experiment is to place the triblock at the interface between PS and PMMA homopolymers. As in the previous case, the sensitivity of the PMMA to the ion beam precluded any quantitative analysis of this system. Results similar to those of the PXE/PMMA case were obtained for PS/PMMA, allowing only the conclusion that the triblock copolymer indeed orders at the interface by adopting a hairpin configuration. A more quantitative assessment of this system is currently underway using neutron reflectivity, where the issue of beam sensitivity is circumvented.

## Conclusions

It has been shown that P(MMA-*b*-S-*b*-MMA) triblock copolymers order at the interface between layers of immiscible polymers and assume a hairpin configuration. In particular, DSIMS studies on triblocks where either the center block or the end blocks are labeled with deuterium have shown that the triblock copolymer orders at the interface between PS/PVC, PXE/PVC, PXE/PMMA, and PS/PMMA. In the first two cases a broadening of the interfacial width is observed with the addition of the triblock copolymer. These four systems encompass cases where favorable interactions exist between one, both, or neither of the block components with the homopolymer layers and suggest that the ordering is a general phenomenon. Also, it has been shown that, for incomplete coverage of the interface by a copolymer, the triblock copolymer is more effective in reducing the interfacial tension than a diblock copolymer of equal molecular weight and com-



position. However, as the concentration is increased, the interfacial activity of the diblock and triblock copolymer is comparable.

**Acknowledgment.** This work was supported in part by the Department of Energy, Office of Basic Energy Sciences, under Contract DE-FG03-88ER45375.

## References and Notes

- (1) Molau, G. E. In *Block Copolymers*; Aggarwal, S. C., Ed.; Plenum Press: New York, 1970.
- (2) Anastasiadis, S. H.; Grancarz, I.; Koberstein, J. T. *Macromolecules* **1989**, *22*, 1449.
- (3) Fayt, R.; Jérôme, R.; Teyssié, Ph. *J. Polym. Sci., Polym. Lett.* **1986**, *24*, 25.
- (4) Ouhadi, T.; Fayt, R.; Jérôme, R.; Teyssié, Ph. *Polym. Commun.* **1986**, *27*, 212.
- (5) Brown, H. R. *Macromolecules* **1989**, *22*, 2859.
- (6) Russell, T. P.; Menelle, A.; Hamilton, W. A.; Smith, G. S.; Satija, S. K.; Majkrzak, C. F. *Macromolecules* **1991**, *24*, 5721.
- (7) Shull, K. R.; Winey, K. I.; Thomas, E. L.; Kramer, E. J. *Macromolecules* **1991**, *24*, 2748.
- (8) Dai, K. H.; Kramer, E. J.; Shull, K. R. *Macromolecules* **1992**, *25*, 220.
- (9) Leibler, L. *Makromol. Chem., Macromol. Symp.* **1988**, *16*, 1.
- (10) Shull, K. R. *J. Chem. Phys.* **1991**, *94*, 5723.
- (11) de Gennes, P.-G. *Macromolecules* **1980**, *13*, 1069.
- (12) Lee, D. C.; Chung, T. C. *J. Polym. Sci., Polym. Chem. Ed.* **1990**, *28*, 505.
- (13) Szwarc, M. *Carbanions, Living Polymers and Electron Transfer Processes*; Wiley-Interscience: New York, 1968.
- (14) Maddams, W. F. *J. Macromol. Sci., Phys.* **1977**, *B14*, 87.
- (15) Composto, R. J.; Kramer, E. J. *J. Mater. Sci.* **1991**, *26*, 2815.
- (16) Boese, D.; Russell, T. P. Unpublished results.
- (17) Sakto, T.; Tsujita, Y.; Takizawa, H.; Kinoshita, T. *Macromolecules* **1991**, *24*, 158.
- (18) Coulon, G.; Russell, T. P.; Deline, V. R.; Green, P. F. *Macromolecules* **1989**, *22*, 2581.
- (19) Hesselink, F.-T. *J. Phys. Chem.* **1969**, *73*, 3488.
- (20) Composto, R. J.; Kramer, E. J.; White, D. M. *Macromolecules* **1988**, *21*, 2580.
- (21) Shull, K. R.; Kramer, E. J. *Macromolecules* **1990**, *23*, 4769.
- (22) Balazs, A. C.; Siemasko, C. P.; Lantman, C. W. *J. Chem. Phys.* **1991**, *94*, 1653.
- (23) Leibler, L. *Macromolecules* **1982**, *15*, 1283.

**Registry No.** P(MMA-*b*-MMA), 106911-77-7; PS, 9003-53-6; PMMA, 9011-14-7; PXE (copolymer), 25134-01-4; PXE (SRU), 24938-67-8; PVC, 9002-86-2.